JOURNAL OF MATERIALS SCIENCE 23 (1988) 2989–2994

Surface micromorphology and dissolution kinetics of potassium dihydrogen phosphate (KDP) crystals in undersaturated aqueous solutions

A. KOZIEJOWSKA, K. SANGWAL*
Institute of Physics, Technical University of Łódź, Wólczańska 219, 93 005 Łódź, Poland

The results of dissolution kinetics and surface micromorphology of (010) and (011) faces of potassium dihydrogen phosphate (KDP) crystals etched in undersaturated aqueous solutions are described. They are then analysed from the standpoint of the theories of dissolution and growth. It was found that Cabrera's mechanism of dislocation etch-pit formation and birth-and-spread model of growth may be applied in the case of dissolution of KDP crystals.

1. Introduction

The process of crystal etching includes, among others, the formation of etch pits at defect sites and the macroscopic dissolution of perfect regions of a surface away from the defect sites [1, 2]. Different theories have been advanced to explain these aspects of the phenomenon of crystal etching [1]. The thermodynamic, spiral dissolution and topochemical adsorption theories are used to explain the formation of etch pits at both screw and edge dislocations; the kinematic theories interpret the morphology of etched surfaces and the terracing of etch pits, and surface nucleation and reaction models describe the kinetics of etching. In the etching literature, however, few investigations have appeared in which an attempt has been made to confront experimental data with theoretical predictions [3–5]. In particular, there is a lack of studies on etching kinetics and on the range of applicability of different theories of etch-pit formation. Such studies necessitate obtaining data on kinetics of etching and the simultaneous observation of the surface micromorphology of etched specimens in a wide range of experimental conditions. In the present paper the experimental results on dissolution kinetics and surface micromorphology of (010) and (011) faces of potassium dihydrogen phosphate (KH_2PO_4, KDP) crystals etched in undersaturated aqueous solutions are described and examined in the light of the theories of growth and etching of crystals.

2. Experimental methods

The crystals for the dissolution experiments were grown at 30° C by the slow solvent evaporation method from aqueous solutions prepared from distilled water and analytical grade KDP. They showed the usual growth habit and were endowed with relatively large prismatic (010) and small pyramidal (011) faces. For experimental purposes, only transparent crystals 8 to 15 mm long in the [001] direction and free from visible inclusions, cracks and dissolution were selected. The density of dislocation etch pits produced on the two types of faces of these crystals by rubbing them with a filter paper wetted with water [6] was about 10^4 cm^{-2}.

For the determination of macroscopic dissolution rate and the investigation of surface dissolution micromorphology, part of the specimen surfaces was masked by dipping it in a dilute (about 5%) solution of plexiglass in acetone and subsequently dried by evaporating the acetone. After the plexiglass coating became firm on the specimens, they were carefully etched for suitable durations in aqueous solutions of different undersaturations. The undersaturation was achieved by raising the temperature of an aqueous solution saturated at 29.6° C. The plexiglass coating was then dissolved in acetone and photographs of the dry etched regions were made. Thereafter the thickness of the dissolved layer was estimated either by using an interference microscope or by focusing an optical microscope on the masked and unmasked areas of the samples. In the case of the former method, the etched specimens were coated with a thin film of aluminium. After determining the thickness of the dissolved layer, the surface was etched to produce dislocation etch pits with a wet filter paper [6]. Subsequently, the previously photographed regions were rephotographed.

The macroscopic dissolution rate was estimated from the thickness of the crystal layer dissolved after a particular time. It was found that the two methods give fairly reproducible results.

* *Permanent address*: Institute of Chemistry, Pedagogical University of Częstochowa, Al. Zawadzkiego 13/15, 42 200 Częstochowa, Poland.

0022–2461/88 $03.00 + .12

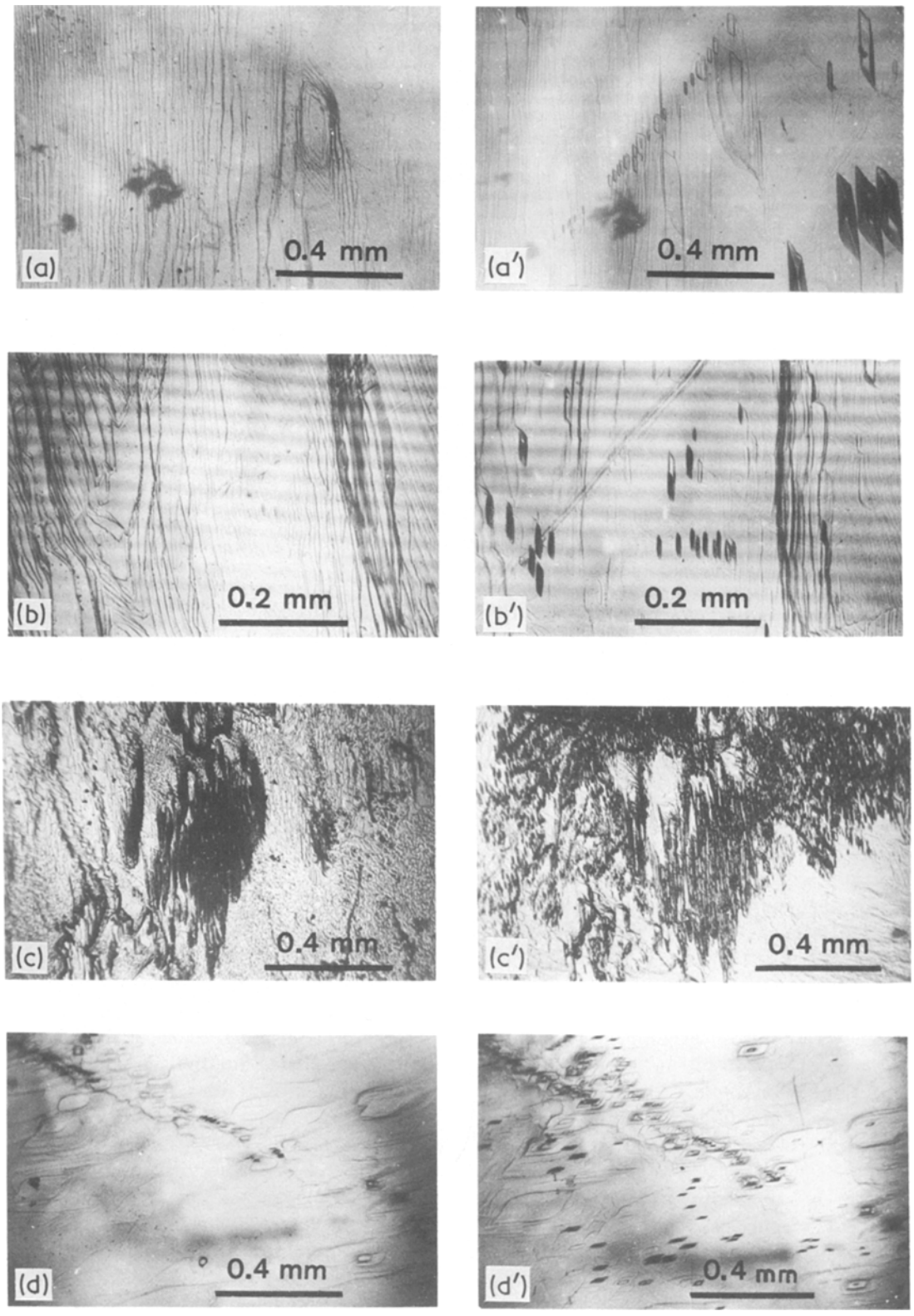

Figure 1 Etch patterns produced on the (010) face of KDP at (a) 2.77, (b) 5.82, (c) 6.93 and (d) 9.70% undersaturation. (a′ to d′) Etch patterns produced in the areas of photographs (a to d) by gently rubbing the surfaces with wet filter papers.

3. Experimental results

The micromorphology of the (010) and (011) surfaces of KDP etched in aqueous solutions at different undersaturations is shown in Figs 1a to d and 2a to e, respectively. The etch-pit patterns produced on the same areas by gently rubbing the surfaces with a filter paper wetted with water are illustrated in Figs 1a′ to d′ and 2a′ to e′, respectively. The following points may be noted from these figures:

(1) At low values of undersaturation the density of

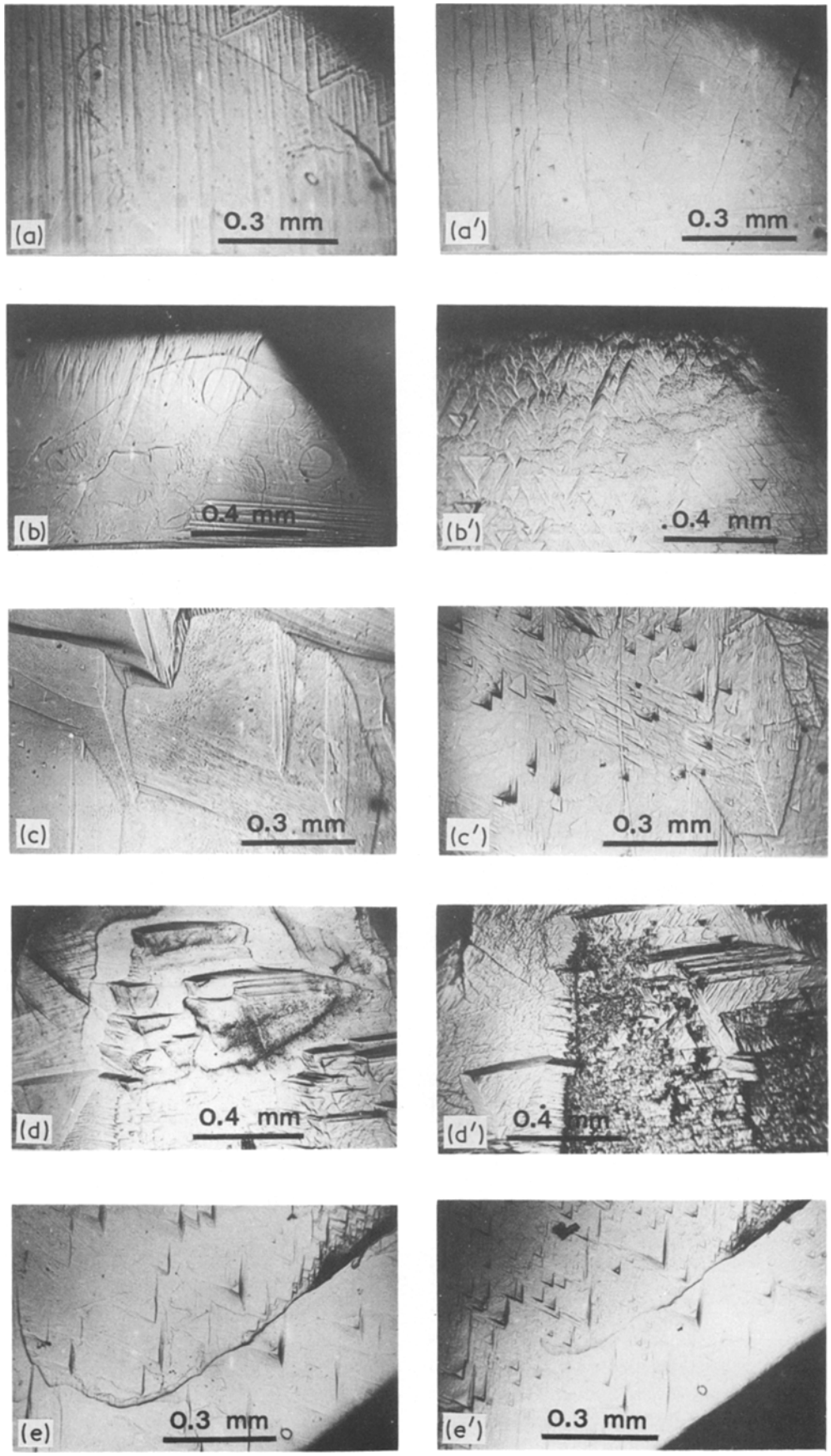

Figure 2 Etch patterns formed on the (011) face of KDP at (a) 1.39, (b) 4.16, (c) 5.82, (d) 6.93 and (e) 9.70% undersaturation. (a′ to e′) Dislocation etch-pit patterns formed in the regions of (a to e) by gently rubbing the surfaces with wet filter papers.

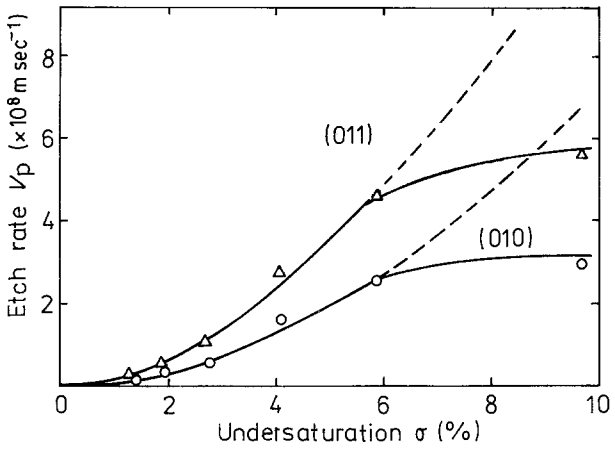

Figure 3 Plots of surface dissolution rate v_p of the (010) and (011) faces of KDP against σ. The full lines represent the experimental data. Except in the range of the highest undersaturation indicated by the dashed lines, the data may be represented by an exponential relation.

etch pits is too low in comparison with that revealed by routine etching. However, at higher undersaturations, most of the dislocations are revealed (compare Figs 1c and d and 2d and e with Figs 1c′ and d′ and 2d′ and e′).

(2) The pit slope, as judged from their contrast, increases with an increase in the undersaturation of the etching solution (Figs 2b to d).

(3) Etching in undersaturated solutions is favoured at the edges of the crystal surfaces. This feature may be easily observed in Figs 2a and b.

(4) Even at low undersaturations some dislocations are revealed, as may be seen from Figs 1b and b′ and 2c and c′. Moreover, the appearance of the etch patterns produced on the (011) face at 2 to 6% unders saturation is similar to that observed on the (111) face of diamond-type crystals [1, 7].

The dependence of surface dissolution rate, v_p, on undersaturation σ (equal to $(c_0 - c)/c_0$ where c and c_0 are the actual and equilibrium solute concentrations in moles per litre at a particular temperature) is presented in Fig. 3. It is obvious that, except for the highest undersaturation, the dependence is exponential in nature.

4. Discussion

Etching of the surface of a crystal in undersaturated solutions and corrosive media usually leads to the formation of etch pits due to localized dissolution at the sites of dislocations and other defects as well as to the overall general surface dissolution. The formation of etch pits at defect sites takes place when the rates of etching normal to the dissolving surface at the defect site, v_n, and away from it in the tangential direction, v_t, and the rate of overall surface dissolution, v_p, satisfy the condition: $v_p < v_n < v_t$. In the case of dislocations, the formation of etch pits may take place either (1) by their spontaneous opening up or (2) by the unwinding of spiral turns of screw dislocations and by a repeated two-dimensional nucleation process favoured by an edge dislocation. The strain energy of edge and screw dislocations is responsible for the spontaneous non-stationary dissolution, but in the latter mechanism involving stationary dissolution it is the geometrical arrangement of atoms/molecules around the dislocation lines rather than the energy localized around them. In Cabrera's model, the transition from stationary dissolution to spontaneous non-stationary fast dissolution takes place at a critical value of undersaturation, σ_c, given by [1–4, 8]

$$\sigma_c = \frac{2\pi^2\gamma^2\Omega}{kTG\boldsymbol{b}^2\alpha} \approx \frac{20\gamma^2\Omega}{kTG\boldsymbol{b}^2} \quad (1)$$

where γ is the surface free energy, Ω the molecular volume, k the Boltzmann constant, T the absolute temperature, G the shear modulus of the crystal, $\boldsymbol{b}$ Burger's vector of a dislocation and α a constant characterizing the dislocation type equal to 1 and $1/(1 - \nu)$ where ν is Poisson's ratio for clean screw and edge dislocations respectively. The radius of the critical two-dimensional nucleus at the dislocation site corresponding to σ_c, is expressed by [1–4, 8]

$$r_c' = \gamma\Omega/2kT\sigma_c \quad (2)$$

where r_c' is the radius of critically sized stable nucleus at a dislocation site and the energy barrier for surface dissolution [1–3, 8] is

$$\Delta G_p^* = \pi h\gamma^2\Omega/kT\sigma_c = 2\pi r_c' h\gamma \quad (3)$$

where ΔG_p^* is the energy barrier for surface dissolution and h the height of a step.

According to Schaarwächter [9], the rate of surface dissolution

$$v_p = K\sigma^{2/3} \exp\left[-(\Delta G_p^* + 3\Delta H)/3kT\right] \quad (4)$$

where ΔH is the free energy change for a molecule going from the crystal surface into the solution and K is a constant.

$$K = h^2\nu\Omega^{-1/3}k^{*2/3} \quad (5)$$

$$\Delta G_p^* = \pi h\gamma^2\Omega/kT\sigma = \pi r_c h\gamma \quad (6)$$

$$r_c = 2r_c' \quad (7)$$

where ν is the frequency factor ($\approx 10^{13}$ sec^{-1}) k^* is the ledge mobility factor $\leqslant 2$ and r_c the radius of critically sized stable nucleus on a perfect surface. If it is assumed that growth theories are also valid for dissolution, then from the BCF surface diffusion model [1, 10, 11]

$$v_p = (C\sigma^2/\sigma_1)\tanh(\sigma_1/\sigma) \quad (8)$$

where C and σ_1 are constants, and from the birth-and-spread (BS) model [1, 11]

$$v_p = A\sigma^{5/6} \exp(-B/\sigma) \quad (9)$$

where A and B are constants:

$$A = 2h^{1/6}\Omega^{5/6}(\bar{v}/\pi)^{1/3}(n_1 D_s\beta\Lambda c_0'/\lambda_s)^{2/3} \quad (10)$$

$$B = \pi h\gamma^2\Omega/3k^2T^2 = \Delta G_p^*\,\sigma/3kT \quad (11)$$

where $\bar{v}$ is the mean velocity of surface-adsorbed molecules equal to $(8kT/\pi m)^{1/2}$ (m is the mass of a molecule of KDP equal to the ratio of its molecular weight to Avogadro number), n_1 is the equilibrium surface density of adsorbed monomers, D_s is the surface diffusion coefficient, β is the retardation factor, $\leqslant 1$ for a straight step, Λ is the kink retardation factor $\leqslant 1$, c_0' is the equilibrium surface concentration

TABLE I Values of parameters used in the calculations

Parameter	Units	Value	Source
c_0	m^{-2}	h^{-2}	–
n_1	m^{-2}	h^{-2}	–
D_s	$nm^2\,sec^{-1}$	1.5×10^7	[12]
Ω	m^3	9.67×10^{-29}	Present work
$\bar{v}$	$m\,sec^{-1}$	2.17×10^2	Present work
h (010)	nm	0.743	[13]
h (011)	nm	0.507	[13]
G	Nm^{-2}	1.26×10^{10}	[14]
m	g	2.26×10^{-22}*	Present work

*It is assumed that a molecule of KH_2PO_4 is the dissolution unit.

of the solute and λ_s is the mean diffusion distance on the surface.

Now we discuss the results of the etching of KDP in the light of the above theoretical background. The micromorphology of the etched surfaces of KDP presented in Figs 1 and 2 suggests that there exists an undersaturation barrier above which dislocation etch pits are easily formed. For the (010) and (011) faces the values of these undersaturations are about 9.0 and 6.4% respectively. The preferred occurrence of dissolution at crystal edges indicates that surface dissolution takes place by surface nucleation process. Consequently, it may be inferred that Cabrera's theory of etch-pit formation holds good in the case of KDP.

The increase of pit slope with undersaturation below σ_c may be explained by a spiral dissolution process [1, 2], Cabrera's model [1, 2] and Schaarwächter's model [1, 2, 9]. However, in the spiral dissolution process screw dislocations are the only active sites for etch-pit formation, while in the Schaarwächter's mechanism both edge and screw dislocations are revealed without a transition from stationary to non-stationary fast dissolution. Thus the formation of block-like patterns on the (011) face of KDP and on the (111) faces of diamond-type crystals, which are in fact, as the present results indicate, due to shallow etch pits at the sites of both edge and screw dislocations, may also be explained by Cabrera's theory, as has been pointed out previously [1].

As observed earlier [1], it was found that the BCF model (Equation 8) is unsatisfactory to represent the present data on dissolution kinetics of KDP. Therefore, in order to analyse the kinetic data, Equations 4 and 9, which are based on two-dimensional surface nucleation, were used. The order of the pre-exponential factors K and A of the two equations was estimated from Equations 5 and 10, respectively, assuming that $h \approx \lambda_s$, $\beta = 1$, $\Lambda = 1$, $k^* = 2$ and $c_0' = n_1 \approx h^{-2}$. The absolute values of different parameters used in the calculations are given in Table I. Thus according to the Schaarwächter and BS models, for the (010) face $K = 1.9 \times 10^4\,m\,sec^{-1}$ and $A = 2.2 \times 10^{-7}\,m\,sec^{-1}$, respectively.

The kinetic data of Fig. 3 were plotted as $\ln (v_p/\sigma^{2/3})$ and $\ln (v_p/\sigma^{5/6})$ against $1/\sigma$ plots, and the constants K and A of Equations 4 and 9 were evaluated from the plots. It was found that for the (010) face $K = 3.1 \times 10^{-7}\,m\,sec^{-1}$ (for $\Delta H = 0$, Equation 4) and $A = 4.5 \times 10^{-7}\,m\,sec^{-1}$. Obviously, there is a large discrepancy in the experimental and theoretical values of K but the experimental value of A agrees well with the estimated value. Therefore it may be concluded that Schaarwächter's theory does not represent the etch rate data satisfactorily, but that the BS model may be applied.

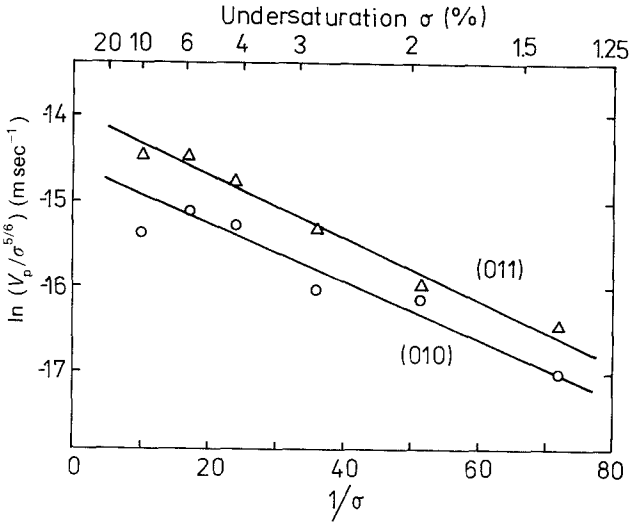

Figure 4 Plots of $\ln (v_p/\sigma^{5/6})$ for the (010) and (011) faces of KDP against $1/\sigma$.

The plots of $\ln (v_p/\sigma^{5/6})$ against $1/\sigma$ representing the BS model for the (010) and (011) faces of KDP are shown in Fig. 4. The values of the constants A (Equation 10) and B (Equation 11) of Equation 9 are given in Table II. The values of critical undersaturation, as judged from the micromorphology of etched surfaces, are also given in this table.

A proof of the validity of Cabrera's theory of etch-pit formation and the BS model to explain the kinetic data is furnished by the value of surface energy γ estimated by using Equations 1 and 11, and that available from other sources. The values of γ were estimated by substituting the values of G from Table I and of B and σ_c from Table II, and taking $b \approx h$ (Table I) in the light of the fact that the direction of a majority of the dislocations in KDP are roughly perpendicular to the (010) and (011) faces [16]. For the estimation of γ from σ_c it was also assumed that $\alpha = 1$. The values of γ are included in Table II.

Joshi and Anthony [15] have studied the dissolution kinetics of the (010) face of KDP up to 35% undersaturation at 20, 30 and 40° C. The values of A, B and γ estimated from their data are also included in Table II. Corresponding to σ_c, r_c' and ΔG_p^* may be calculated by using Equations 7 and 11. These values are given in Table II. From Table II one may note that $r_c' = (0.5 - 1.3)h$. In view of the fact that in our calculations of r_c' we have used the bulk undersaturation, it is reasonable to believe that $r_c' \geqslant h$. This estimate is justified by Cabrera's mechanism of dislocation etch-pit formation.

The values of γ estimated from the data on etch rates and undersaturation barrier are similar. These values of γ agree well with those reported in the literature [17–19]. The agreement in the values of γ obtained by using different approaches implies that

TABLE II Experimental and theoretical values of some parameters

Plane	T(K)	B	A (m sec^{-1})	σ_c	From etch rate data			From undersaturation barrier		
					ΔG_p^* (kJ mol^{-1})	r_c' (nm)	γ (mJ m^{-2})	ΔG_p^* (kJ mol^{-1})	r_c' (nm)	γ (mJ m^{-2})
(011)	303*	0.0390	8.4×10^{-7}	0.064	4.6	0.65	3.6	1.5	0.38	2.1
(010)	293†	0.05289	3.0×10^{-7}	–	–	–	3.4	–	–	–
	303*	0.03343	4.5×10^{-7}	0.090	2.8	0.36	2.8	5.0	0.48	3.7
	303†	0.04083	4.2×10^{-7}	–	–	–	3.1	–	–	–
	313†	0.04767	6.3×10^{-7}	–	–	–	3.4	–	–	–

*Our data. †Data of [15].

Cabrera's theory and the BS model may be used to describe the etching process.

6. Conclusions

The experimental results presented in this work show that in the case of KDP Cabrera's mechanism of dislocation etch-pit formation holds good. The data of the undersaturation dependence of surface dissolution rate, on the other hand, can be satisfactorily explained by the birth-and-spread model of two-dimensional surface nucleation advanced for crystal growth.

Acknowledgements

The authors thank Mr B. Staroń and Dr M. Szurgot for their assistance with the experiments. This work was partially financed under Research Project CPBP 01.20.3.–2.4, and was based on the material presented at the 8th International Conference on Crystal Growth, York, 1986.

References

1. K. SANGWAL, "Etching of Crystals: Theory, Experiment and Application", Series: Defects in Solids, Vol. 15, edited by S. Amelinckx and J. Nihoul (North-Holland, Amsterdam, 1987) Ch. 4.
2. K. SANGWAL and A. A. URUSOVSKAYA, *Prog. Cryst. Growth Character.* **8** (1984) 327.
3. P. BENNEMA and W. J. P. VAN ENCKEVORT, *Ann. Chim. Fr.* **4** (1979) 451.
4. B. VAN DER HOEK, W. J. P. VAN ENCKEVORT and W. H. VAN DER LINDEN, *J. Cryst. Growth* **61** (1983) 181.
5. K. SANGWAL and G. ZANIEWSKA, *J. Mater. Sci.* **19** (1984) 1131.
6. K. SANGWAL, M. SZURGOT, J. KARNIEWICZ and W. KOLASIŃSKI, *J. Cryst. Growth* **58** (1982) 261.
7. W. J. P. VAN ENCKEVORT and L. J. GILING, *ibid.* **45** (1978) 90.
8. N. CABRERA and M. M. LEVINE, *Phil. Mag.* **1** (1956) 450.
9. W. SCHAARWÄCHTER, *Phys. Status Solidi* **12** (1965) 865.
10. W. K. BURTON, N. CABRERA and F. C. FRANK, *Phil. Trans. R. Soc.* **A243** (1951) 299.
11. M. OHARA and R. C. REID, "Modelling Crystal Growth Rates from Solutions" (Prentice-Hall, New Jersey, 1973).
12. M. RAK, *Sci. Bull. Łódź Techn. Univ., Physics* **7** (1984) 25.
13. I. GAJEWSKA, S. PIETRAS, J. RUDZIŃSKA and A. SCHELLENBERG (eds), "Poradnik Fizyko-chemiczny" (Naukowo-Techniczne Press, Warsaw, 1974).
14. K. H. HELLWEGE and A. M. HELLWEGE (eds), "Numerical Data and Functional Relationships in Science and Technology", Group III, Vol. 11 (Springer, Berlin, 1979).
15. M. S. JOSHI and A. V. ANTHONY, *Ind. J. Pure Appl. Phys.* **18** (1980) 479.
16. C. BELOUET, *Prog. Cryst. Growth Character.* **3** (1981) 121.
17. M. S. JOSHI and A. V. ANTHONY, *J. Cryst. Growth* **46** (1979) 7.
18. M. SHANMUGHAM, F. D. GNANAM and P. RAMASAMY, *J. Mater. Sci.* **19** (1984) 2837.
19. K. WOJCIECHOWSKI and W. KIBALCZYC, *J. Cryst. Growth* **76** (1986) 379.

Received 27 April
and accepted 16 December 1987